Delay- and noise-induced transitions: a case study for a Hongler model with time delay

T.D. Frank[1], K. Patanarapeelert[2]. I. M. Tang[3]

[1] *Institute for Theoretical Physics, University of Münster, Wilhelm-Klemm-Str. 9, 48149 Münster, Germany*

[2] *Faculty of Science, Department of Mathematics, Mahidol University, Rama VI Road, Bangkok 10400, Thailand*

[3] *Faculty of Science, Department of Physics, Mahidol University, Rama VI Road, Bangkok 10400, Thailand*

Abstract

Using an exactly solvable model — a generalized Hongler model — we study the impact of time delays on noise-induced transitions to bistability. In particular, we show that systems described by the generalized Hongler model exhibit three parameter regimes. They can be monostable, bistable, or nonstationary. Transitions are induced both by the amplitude of the multiplicative noise and the delay time.

PACS: 05.70.Ln, 05.40.-a, 02.30.Ks

1 Introduction

Open systems that operate far from thermodynamic equilibrium are typically subjected to noise [1]. In particular, when system parameters fluctuate, systems with multiplicative noise sources can be found that exhibit noise-induced

[1] e-mail: tdfrank@uni-muenster.de

transitions [2]. Such multiplicative noise systems may involve time-delayed feedback structures. Prominent examples of systems with time-delayed feedback loops are biological systems, where time delays naturally arise in terms of maturation times, on the one hand, and due to the propagation of energy, matter, and information through the systems, on the other hand (see, e.g., [3–13]). Therefore, in general, when dealing with open systems, we need to take both the impacts of time delays and multiplicative noise sources into account. In particular, for the human movement system this has been explicitly illustrated for the pupil light reflex [14], pointing tasks [15], and balancing movements [16]. In this context, however, exact analytical results can hardly be found in the literature. Some recent studies have been focused on delay systems with linear drift terms and multiplicative noise sources [17] and on the identification of multiplicative noise sources in time-delayed stochastic systems on the basis of experimental data [18]. In contrast, in the present manuscript, we study an exactly solvable model that involves a nonlinear drift force, multiplicative noise, and a time delay. To this end, we will discuss a generalized Hongler model with time delay. Since the proposed generalized Hongler model can be solved analytically (at least with respect to the stationary first order statistics), it can be regarded as a benchmark model that might be used to check numerical algorithms and approximative analytical approaches (e.g. perturbation theoretical approaches to time-delayed stochastic systems [19]).

2 Hongler model with time delay

2.1 Analytical results

With start off with the Hongler model without delay given by the Langevin equation [2,20,21]

$$\frac{\mathrm{d}}{\mathrm{d}t}X(t) = -\gamma \tanh(cX) + \frac{\sqrt{Q}}{\cosh(cX)}\Gamma(t) \ , \tag{1}$$

where $X(t)$ denotes a state variable defined on the phase space $\Omega = \mathbb{R}$ and $\gamma, c, Q > 0$ are parameters. Here, $\Gamma(t)$ describes a Langevin force normalized to $\langle \Gamma(t)\Gamma(t') \rangle = \delta(t - t')$, where $\langle \cdots \rangle$ denotes an ensemble average and $\delta(\cdot)$ is the Dirac delta function [22]. The expression $\sqrt{Q}\Gamma(t)/\cosh(cX)$ describes a multiplicative noise source. Accordingly, we interpret the scalar parameter Q as a noise amplitude. Next, we derive from Eq. (1) a stochastic model involving a time-delayed feedback. Let X_τ denote the time-delayed state variable $X_\tau(t) = X(t-\tau)$. Furthermore, recall that we have $\tanh(z) = \sinh(z)/\cosh(z)$. Then, in line with Eq. (1), we define a Hongler model with delay by means of the stochastic delay differential equation

$$\frac{\mathrm{d}}{\mathrm{d}t}X(t) = -\gamma \frac{\sinh(cX_\tau)}{\cosh(cX)} + \frac{\sqrt{Q}}{\cosh(cX)}\Gamma(t) \ . \tag{2}$$

As we will show in the following, this stochastic model is a powerful tool to study the interplay between impacts of time delays and multiplicative noise sources because it features delay- and noise-induced transitions, on the one hand, and can be solved analytically, on the other hand. Note that in what follows the noise term will be interpreted according to the Stratonovich calculus [23].

Now, let us examine Eq. (2) in detail. Using the variable transformation

$$Y(t) = \frac{\sinh(cX(t))}{c} \ , \tag{3}$$

we can transform Eq. (2) into the linear stochastic delay differential equation

$$\frac{\mathrm{d}}{\mathrm{d}t}Y(t) = -\gamma c Y(t-\tau) + \sqrt{Q}\,\Gamma(t) \ . \tag{4}$$

The stationary probability density $P_{\mathrm{st}}(y) = \langle \delta(y - Y(t)) \rangle$ of Eq. (4) is given by the Gaussian distribution

$$P_{\mathrm{st}}(y) = \frac{1}{\sqrt{2\pi K}} \exp\left\{ -\frac{y^2}{2K} \right\} \tag{5}$$

involving the variance $K = K(Q, \tau, \gamma c)$ [24–26]. In particular, for $\tau = 0$ Eq. (4) describes an Ornstein-Uhlenbeck process, which implies that [22]

$$K(Q, 0, \gamma c) = \frac{Q}{2\gamma c} \ . \tag{6}$$

For $\tau > 0$ but $\tau < \tau_c = \pi/(2\gamma c)$ we have [24–26]

$$K(Q, \tau, \gamma c) = \frac{Q}{2\gamma c} \, \frac{1 + \sin(\gamma c \tau)}{\cos(\gamma c \tau)} \ . \tag{7}$$

At the critical parameter value $\tau = \tau_c$ there is a Hopf bifurcation such that for $\tau > \tau_c$ there does not exist a stationary distribution. For $\tau > \tau_c$ the first moment $\langle Y \rangle$ oscillates with an exponentially growing amplitude [27] (see also [28] for the deterministic case). Using the backwards transformation $Y \to X$, the probability distribution $P_{\mathrm{st}}(x) = P_{\mathrm{st}}(y)|\mathrm{d}y/\mathrm{d}x|$ is given by

$$P_{\mathrm{st}}(x) = \frac{\cosh(cx)}{\sqrt{2\pi K}} \exp\left\{ -\frac{\sinh^2(cx)}{2c^2 K} \right\} \tag{8}$$

with K defined by Eq. (7). That is, $P_{\mathrm{st}}(x)$ reads explicitly

$$P_{\rm st}(x) = \sqrt{\frac{\gamma c \cos(\gamma c\tau)}{\pi Q[1+\sin(\gamma c\tau)]}}\cosh(cx)\exp\left\{-\frac{\gamma\cos(\gamma c\tau)}{Qc[1+\sin(\gamma c\tau)]}\sinh^2(cx)\right\} \tag{9}$$

for $\tau \in [0, \tau_c)$. The Hopf bifurcation with respect to the y-coordinate system carries over to the x-coordinate system. Therefore, for $\tau > \tau_c$ our model (2) does not exhibit stationary distributions.

Let us study now the transition to bistability known from the original Hongler model (1) [2,20], which is a transition from a unimodal distribution centered at the origin to a bimodal symmetrical distribution. The unimodal distribution reflects a monostable system. In this context, the state $x = 0$, which is most probably state, may be regarded as a non-exited state. The bimodal symmetrical distribution reflects a bistable system. The states corresponding to the two peaks of this distribution may be interpreted as excited states. Consequently, the transition to bistability may be interpreted as a transition in which a non-excited system becomes an excited system. In order to study the transition to bistability, we need to determine the extrema of $P_{\rm st}(x)$. From $\mathrm{d}P_{\rm st}(x)/\mathrm{d}x = 0$ and Eq. (8) it follows that

$$0 = \sinh(cx)\left[1 - \frac{1}{c^2 K}\cosh^2(cx)\right] \ . \tag{10}$$

From Eq. (10) it is clear that for all parameter values there is an extremum at the origin: $x = 0 \Leftrightarrow \sinh(cx) = 0$. In addition, there are two extrema satisfying $c\sqrt{K} = \cosh(cx)$ provided that the inequality $c\sqrt{K} > 1$ holds. Finally, we can show that for $c\sqrt{K} < 1$ the extremum at $x = 0$ corresponds to a maximum of $P_{\rm st}(x)$, whereas for $c\sqrt{K} > 1$ the distribution $P_{\rm st}(x)$ has a minimum at $x = 0$ and maxima at the two symmetric solutions of $c\sqrt{K} = \cosh(cx)$. Therefore, critical parameters for the transition point are given by

$$K = 1/c^2 \ . \tag{11}$$

At this point, we would like to mention that by rescaling the time variable t and the state variable X in Eq. (2), we can eliminate two of the four parameters of the model. Therefore, it is sufficient to discuss the bifurcation diagram of Eq. (2) in a two-dimensional parameter space. Accordingly, we will use τ, Q as free parameters while we assume that γ, c assume fixed values. Then, the constraint $K = 1/c^2$ describes a bifurcation line in parameter space given by Q, τ. The bifurcation line is given by $Q^* = Q^*(\tau)$ with

$$K(Q^*(\tau), \tau, \gamma, c) = 1/c^2 \ . \tag{12}$$

Substituting Eq. (7) into Eq. (12), we obtain

$$Q^*(\tau) = \frac{2\gamma}{c} \frac{\cos(\gamma c \tau)}{1 + \sin(\gamma c \tau)} \ . \tag{13}$$

We see that the implication $\tau = 0 \Rightarrow Q^* = 0$ holds. Furthermore, we have

$$\frac{\mathrm{d}Q^*}{\mathrm{d}\tau} = -\frac{2\gamma^2}{1 + \sin(\gamma c \tau)} < 0 \tag{14}$$

for $\tau \in [0, \tau_c)$. Finally, for $\tau \to \tau_c = \pi/(2\gamma c)$ we have $Q^* \to 0$. In sum, we arrive at the bifurcation diagram shown in Fig. 1. From Fig. 1 we read off that the transition to bistability can be induced by increasing the noise amplitude Q or the delay τ. That is, in contrast to the original Hongler model (1), the delay Hongler model (2) describes both noise-induced and delay-induced transitions to bistability.

Fig. 1 about here.

2.2 Numerics

Let us illustrate our results for the case $\gamma = c = 1$. In order to solve Eq. (2) numerically, we first transform the Stratonovich stochastic delay differential

equation into the corresponding Ito equation using the relation [23]:

$$\underbrace{g(x)\Gamma}_{\text{Stratonovich}} = \underbrace{g(x)\Gamma}_{\text{Ito}} + \frac{1}{4}\frac{\mathrm{d}}{\mathrm{d}x}g^2 \ . \tag{15}$$

Thus, for $\gamma = c = 1$ we obtain the Ito stochastic delay differential equation

$$\frac{\mathrm{d}}{\mathrm{d}t}X(t) = -\frac{\sinh(X_\tau)}{\cosh(X)} - \frac{Q}{2}\frac{\sinh(X)}{\cosh^3(X)} + \frac{\sqrt{Q}}{\cosh(X)}\Gamma(t) \ . \tag{16}$$

Eq. (16) can be discretized using an Euler forward scheme that reads

$$X_{n+1} = X_n - \Delta t\left[\frac{\sinh(X_{n-m})}{\cosh(X_n)} + \frac{Q}{2}\frac{\sinh(X_n)}{\cosh^3(X_n)}\right] + \frac{\sqrt{Q\Delta t}}{\cosh(X_n)}w_n \ , \tag{17}$$

where time is measured in single time steps Δt like $t = n\Delta t$ and the delay is regarded as a multiple of Δt like $\tau = m\Delta t$ (with $m \geq 0$ integer). Here, w_n are Gaussian distributed random variables with $\langle w_n w_n' \rangle = \delta_{nn'}$ [22].

2.2.1 Delay- and noise-induced transition

For $\gamma = c = 1$ Eq. (9) becomes

$$P_{\mathrm{st}}(x; Q, \tau) = \sqrt{\frac{\cos(\tau)}{\pi Q[1+\sin(\tau)]}}\cosh(x)\exp\left\{-\frac{\cos(\tau)}{Q[1+\sin(\tau)]}\sinh^2(x)\right\} \ . \tag{18}$$

Let us consider a fixed time delay τ with $\tau < \tau_c = \pi/2$. Then, the critical noise amplitude is given by $Q^* = 2\cos(\tau)/[1+\sin(\tau)]$ and can be used to distinguish between the monostable case $Q < Q^*$ (non-excited system) and the bistable case $Q > Q^*$ (excited system). Figure 2 shows examples of $P_{\mathrm{st}}(x)$ for the monostable case (left panel) and the bistable case (right panel) as computed from the analytical solution (18) (solid lines) and as obtained by solving the stochastic evolution equation (17) (diamonds).

Fig. 2 about here.

2.2.2 Hopf bifurcation

Now, let us study the evolution of the first moment $M_1(t) = \langle X(t) \rangle$. Given a fixed noise amplitude Q, we distinguish between the stationary regime with $\tau < \tau_c$ in which $M_1(t)$ converges to a stationary value and the nonstationary regime with $\tau > \tau_c$ in which $M_1(t)$ exhibits an oscillatory behavior. Figure 3 shows M_1 computed from Eq. (17) for the stationary case (left panel) and the nonstationary case (right panel). Note that the amplitude of the oscillation increases monotonically such that the amplitude of the oscillation shown in the right panel of Fig. 3 tends to infinity for $t \to \infty$.

Fig. 3 about here.

3 Conclusions

We have supplemented the Hongler model with a time-delayed feedback in order to study the impact of time delays on noise-induced transitions. We have found that there is a critical bifurcation line $Q^*(\tau)$ in the parameter space spanned by the delay τ and the noise amplitude Q. This bifurcation line separates monostable, non-exited systems from bistable, excited systems. Transitions take place when the delay or the noise amplitude is increased beyond this bifurcation line. Moreover, we have demonstrated that in addition to these stationary parameter regimes there is another parameter regime for which systems described by the generalized Hongler model are nonstationary. The nonstationary behavior emerges via a delay-induced Hopf bifurcation. In sum, the bifurcation diagram is composed of three different parameter regimes. In particular, when the noise amplitude Q is fixed for $Q < 2\gamma/c$ and the delay is gradually increased then there are two kinds of transitions. For small delays the system is monostable and shows an overall non-excited behavior. For moderate delays the system is bistable and can most probably found in

excited states. For large delays the system is unstable in the sense that it exhibits a nonstationary behavior.

The focus of our study was on the first order statistics. Further insights into the interplay between time delays and noise-induced transitions to bistability may be derived by studying quantities of second order statistics. In the context of the Hongler model (1) without delay, second order statistical quantities such as mean first passage times derived from Green's functions and eigenvalues of Fokker-Planck operators have been examined [21]. In principle, similar considerations could be carried out for the time-delayed version of the Hongler model given by Eq. (2). So far, however, closed forms of Fokker-Planck operators and the corresponding Green's functions for stochastic delay differential equations such as Eq. (2) have not been derived (only non-closed forms of Fokker-Planck operators are available by now, see e.g. [19,29]). Therefore, future efforts may be centered around the derivation of closed forms of Fokker-Planck operators for stochastic systems with time delays. These closed forms could be used to study properties of second order statistics and Green's functions, in general, and mean field passage times and eigenvalues of eigenfunction expansions, in particular.

References

[1] H. Haken, *Synergetics: Itroduction and Advanced topics* (Springer, Berlin, 2004).

[2] W. Horsthemke and R. Lefever, *Noise-induced transitions* (Springer, Berlin, 1984).

[3] G. A. Bocharov and F. A. Rihan, J. Comput. Appl. Math. **125**, 183 (2000).

[4] J. M. Cushing, *Integrodifferential equations and delay models in population dynamics* (Springer, Berlin, 1977).

[5] M. C. Mackey and L. Glass, Science **197**, 287 (1977).

[6] H. Sompolinsky, D. Golomb, and D. Kleinfeld, Phys. Rev. A **43**, 6990 (1991).

[7] P. Tass, J. Kurths, M. G. Rosenblum, G. Guasti, and H. Hefter, Phys. Rev. E **54**, R2224 (1996).

[8] V. K. Jirsa and J. A. S. Kelso, Phys. Rev. E **62**, 8462 (2000).

[9] P. W. Nelson, J. D. Murray, and A. S. Perelson, Math. Biosciences **163**, 201 (2000).

[10] H. Haken, *Brain dynamics* (Springer, Berlin, 2002).

[11] A. Hutt, M. Bestehorn, and T. Wennekers, Network: Comput. Neural. Syst. **14**, 351 (2003).

[12] M. G. Rosenblum and A. S. Pikovsky, Phys. Rev. Lett. **92**, 114102 (2004).

[13] K. Patanarapelert and I. M. Tang, Effect of time delay on the transmission of Dengue fever, submitted.

[14] A. Longtin, J. G. Milton, J. E. Bos, and M. C. Mackey, Phys. Rev. A **41**, 6992 (1990).

[15] K. Vasilakov and A. Beuter, J. Theo. Biol. **165**, 389 (1993).

[16] J. L. Cabrera and J. G. Milton, Phys. Rev. Lett. **89**, 158702 (2002).

[17] T. D. Frank, Phys. Rev. E **69**, 061104 (2004).

[18] T. D. Frank, P. J. Beek, and R. Friedrich, Phys. Lett. A **328**, 219 (2004).

[19] T. D. Frank, Phys. Rev. E, Delay Fokker-Planck equations, perturbation theory, and data analysis for nonlinear stochastic systems with time delays, in press; http://pauli.uni-muenster.de/∼tdfrank/tdf04bpert.pdf.

[20] M. Hongler, Helv. Phys. Acta **52**, 280 (1979).

[21] C. R. Doering, Phys. Rev. A **34**, 2564 (1986).

[22] H. Risken, *The Fokker-Planck equation — Methods of solution and applications* (Springer, Berlin, 1989).

[23] T. D. Frank, Phys. Rev. E **66**, 011914 (2002).

[24] U. Küchler and B. Mensch, Stochastics and stochastic reports **40**, 23 (1992).

[25] T. D. Frank and P. J. Beek, Phys. Rev. E **64**, 021917 (2001).

[26] T. D. Frank, P. J. Beek, and R. Friedrich, Phys. Rev. E **68**, 021912 (2003).

[27] M. C. Mackey and I. G. Nechaeva, Phys. Rev. E **52**, 3366 (1995).

[28] J. K. Hale and S. M. V. Lunel, *Introduction to functional differential equations* (Springer, Berlin, 1993).

[29] S. Guillouzic, I. L' Heureux, and A. Longtin, Phys. Rev. E **59**, 3970 (1999).

Figure captions:

Fig. 1: Bifurcation diagram of the Hongler model with time-delayed feedback given by Eq. (2). There are two bifurcation lines separating (i) monostable, non-excited systems described by unimodal distributions, (ii) bistable, excited systems that are described by bimodal distributions, and (iii) unstable systems for which stationary distributions do not exist.

Fig. 2: Illustration of the transition to bistability described by the Hongler model (2). *Panel (a)*: unimodal distribution computed from the distribution (18) (solid lines) and the delay Langevin equation (17) (diamonds) for $Q < Q^*(\tau)$ with $Q = 0.2$, $\tau = 0.5$, $Q^*(0.5) = 1.2$ ($\Delta t = 0.01$, $P_{\rm st}$ was computed from $N = 10^6$ realizations). *Panel (b)*: bimodal distribution computed from the distribution (18) (solid lines) and the delay Langevin equation (17) (diamonds) for $Q > Q^*(\tau)$ with $Q = 2.0$ and $\tau = 0.5$ ($\Delta t = 0.01$, $N = 10^6$).

Fig. 3: Illustration of the Hopf bifurcation described by the Hongler model (2). *Panel (a)*: evolution of $M_1(t)$ in the stable case for $\tau < \tau_c$, $M_1(0) = 0.1$, and parameters as in panel (a) of Fig. 2. *Panel (b)*: evolution of $M_1(t)$ in the unstable case for $\tau > \tau_c$, $M_1(0) = 0.1$, and $Q = 0.2$, $\tau = 2$, $\tau_c = \pi/2 \approx 1.57$ ($\Delta t = 0.01$, $N = 10^6$).

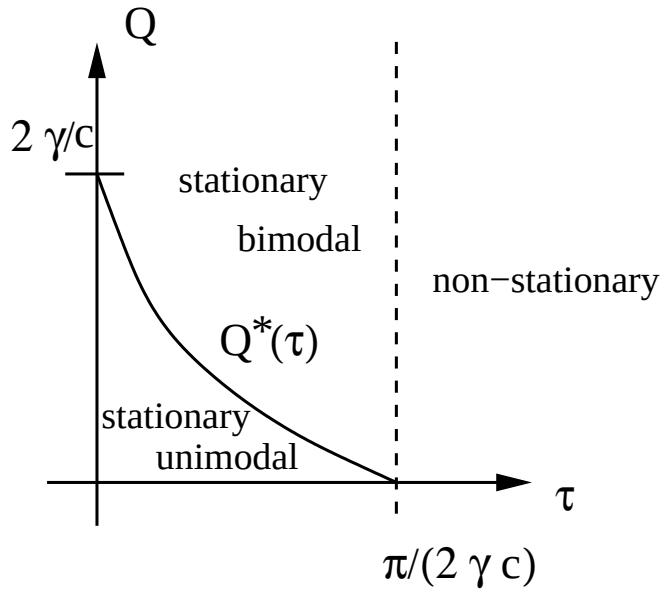
Q
2 γ/c
stationary
bimodal
non−stationary
Q*(τ)
stationary
unimodal
τ
π/(2 γ c)

Fig. 1.

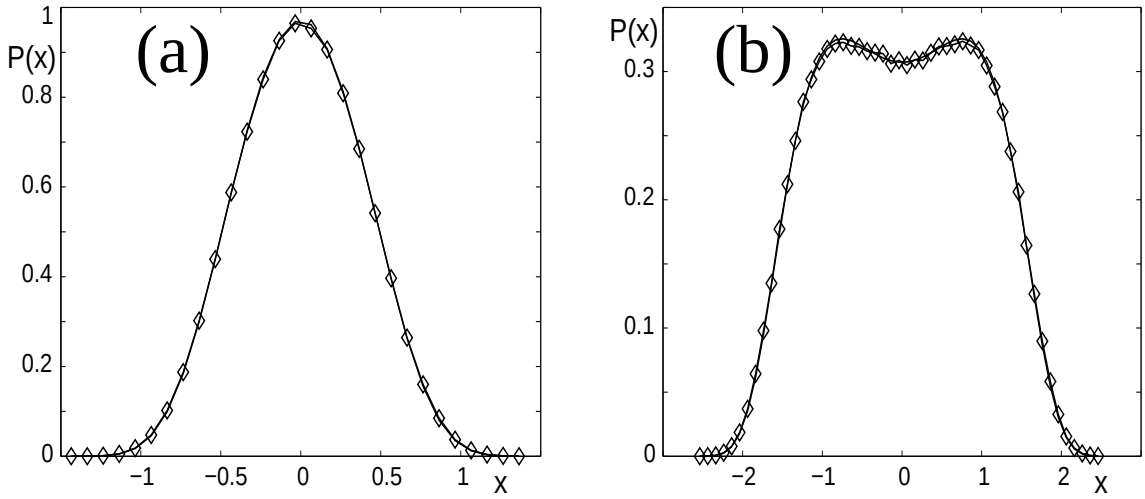
(a)
P(x)
1
0.8
0.6
0.4
0.2
0
−1
−0.5
0
0.5
1
x
(b)
P(x)
0.3
0.2
0.1
0
−2
−1
0
1
2
x

Fig. 2.

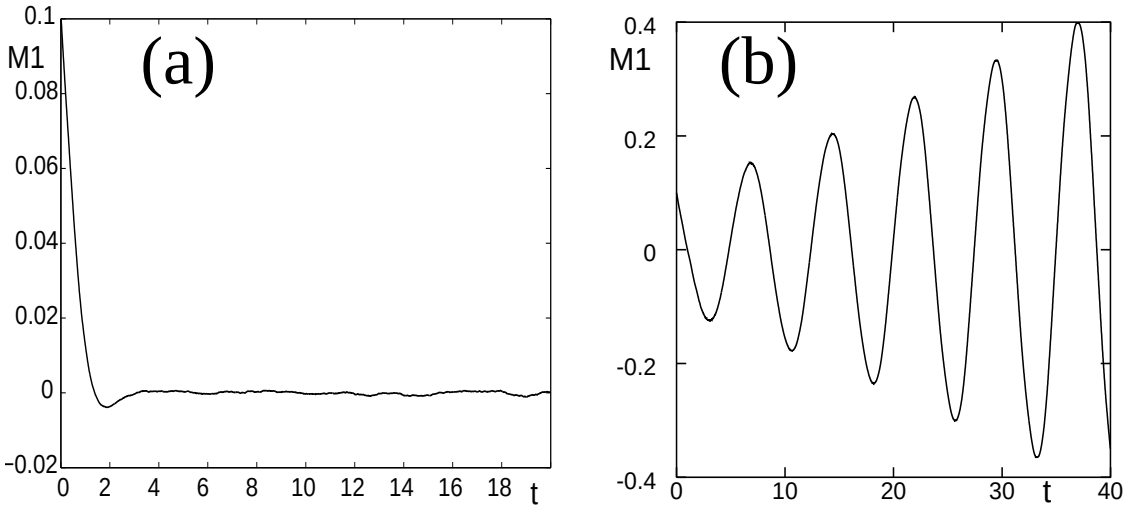
(a)
M1
0.1
0.08
0.06
0.04
0.02
0
-0.02
0 2 4 6 8 10 12 14 16 18 t
(b)
M1
0.4
0.2
0
-0.2
-0.4
0 10 20 30 t 40

Fig. 3.